Proceedings of the Sixth International Conference on
Railway Technology: Research, Development and Maintenance
Edited by: J. Pombo
Civil-Comp Conferences, Volume 7, Paper 16.1
Civil-Comp Press, Edinburgh, United Kingdom, 2024
ISSN: 2753-3239, doi: 10.4203/ccc.7.16.1

The Stability Behaviour of an Electromagnetically Suspended Hyperloop Vehicle Subject to Aeroelastic Forcing

J. Paul, A. B. Fărăgău, R. J. van Leijden, A. V. Metrikine and K. N. van Dalen

**Department of Engineering Structures, Faculty of CEG,
TU Delft
Netherlands**

Abstract

In this paper, we delve into the dynamics of an electromagnetically suspended mass from a rigid support. The study employs a 1.5-degrees-of-freedom system which serves as a simplified model for a Hyperloop vehicle traveling in a tube. Through linear stability analysis, we analytically uncover three distinct regions for the physically significant equilibrium point. Further inspection reveals that the system exhibits limit-cycle vibrations in one of these regions. Employing the harmonic balance method, we determine the properties of the limit cycle, thus unravelling the frequency and amplitude characterizing the periodic oscillations of system's variables. We also present preliminary findings regarding the influence of the steady aeroelastic force on the stability of the system.

Keywords: Hyperloop, electro-magnetic suspension, aeroelastic force, stability, supercritical Hopf bifurcation, harmonic balance, limit cycle.

1 Introduction

The Hyperloop is expected to revolutionize transportation, blending the advantages of aircraft and next-generation rail. This unique fusion yields a richer engineering landscape, presenting an open field for research. While the aeroelastic stability of aircrafts on the one hand and the stability of moving objects in direct (i.e., mechanical) contact with slender beams/rails on the other hand have been extensively studied, the realm of modern rail systems employing magnetic levitation at very high speeds remains largely unexplored. In the context of a Hyperloop vehicle traveling within a

depressurized tube, suspended or levitated electromagnetically from a flexible beam, the potential for integrating the aforementioned mechanisms arises. However, whether these stability mechanisms complement or counteract each other remains to be seen. Noteworthy previous literature pertaining to each individual mechanism is cited below.

It is widely recognized that when a vehicle move along a flexible guideway, oscillations can become unstable if its speed exceeds a specific critical threshold [1]. Metrikine [2] demonstrated that instability arises due to the energy associated with the radiation of anomalous Doppler waves, which feedback energy into the vehicle's vibration through the guideway's reaction force, surpassing that of normal Doppler waves. Identifying such a critical velocity during the design phase is imperative [3].

The primary aeroelastic effects that could impact a Hyperloop vehicle include galloping, fluttering, and vortex-induced vibrations [4,5], although they overlap to some extent. While studies on galloping and fluttering in railway systems exist, most listed studies are focused on detailed computational fluid dynamics analyses [6].

Moreover, several intriguing studies have delved into electromagnetic stability, some of which are referenced herein. Yabuno et al. [7] investigated electromagnetic levitation under base excitation, representing one of the early works in this area, while Inoue et al. explored the same system with excitation on the mass, employing linear PD control [8]. The work represents another attempt to explore a very similar model, but for parametric instability.

An initial exploration of the combination of the two potentially destabilizing forces, the beam's reaction force and the electromagnetic force, was conducted by Fărăgău et al. [9]. The study determined the stability region in terms of control parameters and the effect of the movement of the moving vehicle on it. The study also identified limit cycles in a specific region of the control parameter plane. The present work endeavours to analyse instability due to a combination of the electromagnetic and aeroelastic forces. A more simplified, 1.5-degrees-of-freedom system is used here (i.e., no flexible but rigid support), as it is analytically more tractable. The investigation focuses on the case in which the aeroelastic force creates an instability and the system thus undergoes galloping. The study derives closed-form expressions for the system's response utilizing the harmonic balance method, to delineate stability boundaries and the presence of limit cycles. Validation of the results is performed through numerical integration using standard MATLAB packages.

The paper is structured as follows: Section 2 presents the model, Section 3 conducts linear stability analysis and Section 4 explores the existence of the limit cycle.

2 Problem statement

Figure 1 illustrates the considered model, representing a simplified model of a Hyperloop vehicle of mass m suspended from a fixed support through the electromagnetic force F.

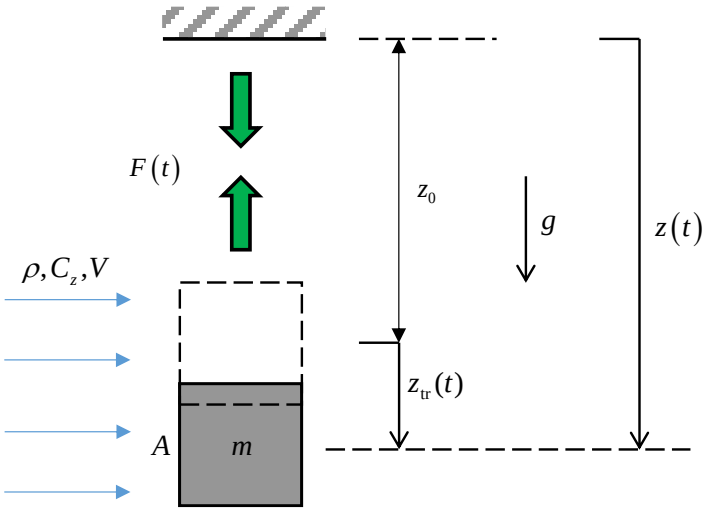

Figure 1: Model of electromagnetically suspended mass subject to air flow.

The equations of motion (EoM), which is Newton's second law, and the equation for electric current that includes a voltage control (i.e., PD control) are defined as follows:

$$m\ddot{z}(t) = -C\frac{I(t)^2}{z(t)^2} + mg + \mu\dot{z}(t) \tag{1}$$

$$\mu = \frac{1}{2}\rho A\left(\frac{\partial C_z}{\partial \alpha}\right)_{\alpha=0} V \tag{2}$$

$$\dot{I}(t) + \frac{z(t)}{2C}\left(\frac{u_0}{I_0} - 2C\frac{\dot{z}(t)}{z(t)^2}\right)I(t) = \frac{z}{2C}\left(u_0 + K_\mathrm{p}(z(t) - z_0) + K_\mathrm{d}\dot{z}(t)\right) \tag{3}$$

The system operates within a gravitational field, experiencing downward acceleration g due to gravity. The desired fixed gap between the vehicle and support, denoted by z_0, corresponds to one of the fixed points with respective steady-state voltage u_0 and current I_0 (see Section 3). The electromagnetic force $F(t)$ between the support and vehicle depends on the displacement $z(t)$ and current $I(t)$ variables. The voltage controls the electromagnet (i.e., the current) to maintain the gap as constant as possible, with control parameters K_p and K_d. C is a constant determined by electromagnet properties. The destabilizing term $\mu\dot{z}$ in Eq. (1) represents the steady aeroelastic force, with μ being the product of all aeroelastic constants. Here, α denotes the relative angle between wind velocity V and vertical component of the

vehicle velocity $\dot{z}$, ρ is the air density, A is the vehicle's cross-sectional area affected by wind, and $C_z(\alpha) = C_L(\alpha) + C_D(\alpha)$, where $C_L(\alpha)$ denotes the lift coefficient and $C_D(\alpha)$ the drag coefficient. For galloping, a straightforward derivation of the destabilizing term $\mu\dot{z}$ is given in [4]. While μ is not a constant in real situations, the maximum oscillation amplitude of the vehicle, typically in the millimetre range, justifies the assumption due to minimal angle change of time.

3 Linear stability analysis

This section undertakes linear stability analysis of the system. The usual approach involves linearizing Eqs. (1) and (3), and deriving eigenvalues of the Jacobian matrix obtained from the linearized equation set at the desired fixed point. Initially, fixed points are determined by considering equilibrium or steady states. The equilibrium state, where all time derivatives are zero, is described by the following set of algebraic equations:

$$\begin{aligned} &C\frac{I^2}{z^2} = \frac{I_0^2}{z_0^2} \\ &\frac{z}{2C}\frac{u_0}{I_0}I = \frac{z}{2C}\left(u_0 + K_p(z - z_0)\right) \end{aligned} \tag{4}$$

Solving Eq. (4) results in two fixed points:

$$\begin{aligned} &z_{ss}^a = z_0;\ I_{ss}^a = I_0 \\ &z_{ss}^b = \frac{-z_0\left(u_0 - K_p z_0\right)}{u_0 + K_p z_0};\ I_{ss}^b = \frac{I_0\left(u_0 - K_p z_0\right)}{u_0 + K_p z_0} \end{aligned} \tag{5}$$

For the second fixed point, either z_{ss}^b or $I_{ss_2}^b$ must be negative, rendering it a nonphysical equilibrium point, especially for systems like the Hyperloop. Hence, for subsequent analyses, only the fixed point $z_{ss}^a = z_0;\ I_{ss}^a = I_0$ is considered.

The next step is to derive the linearized equations. Assuming perturbations around the variables as $z = z_0 + z_{tr}(t)$ and $I(t) = I_0 + I_{tr}(t)$ (the subscript "tr" denotes transient), and applying Taylor series expansions up to and including first order yields

$$\begin{aligned} &m\ddot{z}_{tr} = -2C\frac{I_0}{z_0^2}I_{tr} + 2C\frac{I_0^2}{z_0^3}z_{tr} \\ &\dot{I}_{tr} = -\frac{z_0 R}{2C}I_{tr} + \frac{z_{ss}K_p}{2C}z_{tr} + \frac{(K_d z_0^2 + 2CI_0)}{2z_0 C}\dot{z}_{tr} \end{aligned} \tag{6}$$

The Jacobian of Eq. (6) at the fixed point-a is defined when Eq. (6) is written in state-space form:

$$\frac{d}{dt}\begin{pmatrix} z_{\mathrm{tr}}(t) \\ \dot{z}_{\mathrm{tr}}(t) \\ I_{\mathrm{tr}}(t) \end{pmatrix} = \begin{pmatrix} 0 & 1 & 0 \\ \dfrac{2CI_0^{\,2}}{mz_0^{\,3}} & \dfrac{\mu}{m} & -\dfrac{2CI_0}{mz_0^{\,2}} \\ \dfrac{K_{\mathrm{p}}z_0}{2C} & \dfrac{K_{\mathrm{d}}z_0}{2C}+\dfrac{I_0}{z_0} & -\dfrac{u_0z_0}{2CI_0} \end{pmatrix} \begin{pmatrix} z_{\mathrm{tr}}(t) \\ \dot{z}_{\mathrm{tr}}(t) \\ I_{\mathrm{tr}}(t) \end{pmatrix} \tag{7}$$

The characteristic polynomial of the Jacobian given in Eq. (7) is

$$\lambda^3 - \left(\frac{u_0z_0}{2CI_0} - \frac{\mu}{m}\right)\lambda^2 - \left(\frac{K_{\mathrm{d}}I_0}{mz_0} - \frac{\mu u_0z_0}{2CI_0m}\right)\lambda + \frac{I_0(u_0 - K_{\mathrm{p}}z_0)}{mz_0^{\,2}} = 0 \tag{8}$$

The eigenvalues for each of the fixed points are shown in Figure 2 (i.e., also for fixed point-b). Stability transitions can be obtained from the zero crossings of the real parts of the eigenvalues.

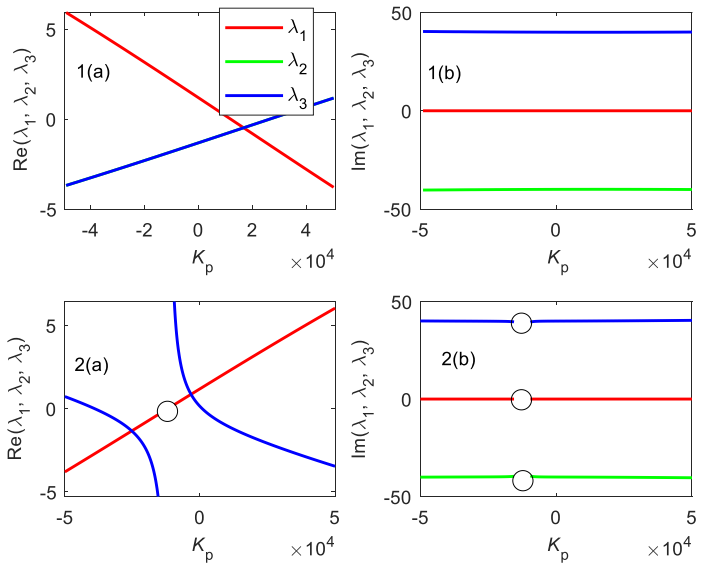

Figure 2: The eigenvalues for each of the fixed points are shown here, figures 1 and 2 represent first and second fixed points, respectively. (a) and (b) represent real and imaginary parts of the eigenvalues, respectively. The small circles in 2 represent singularities. Here,

$K_{\mathrm{d}} = 10000\,(\mathrm{Vs/m}),\ C = 0.05\,(\mathrm{Nm^2/A^2}),\ z_0 = 0.015\,(\mathrm{m}),\ m = 7650\,(\mathrm{kg})$.

Utilizing properties of cubic polynomials, the stability boundaries of the system can be determined. The discriminant of the polynomial suggests that the roots contain one real and two complex conjugates (not shown here). A stability transition requires at least one eigenvalue's real part to be zero (sign change), suggesting two possibilities: the real part of the complex conjugates is zero, or the real root is zero.
In the first scenario, for a polynomial $\lambda^3 + a\lambda^2 + b\lambda + c = 0$ to have one real root and two purely imaginary roots, the relation $ab = -c$ is required, resulting in the first stability transition which is a straight line in the K_p - K_d plane (see Figure 3):

$$K_\mathrm{p} = \frac{u_0}{z_0} + \frac{2CI_0\mu^2 u_0 z_0^3 - m\mu u_0^2 z_0^4}{4C^2 I_0^3 m z_0} + \frac{2CI_0^2 m u_0 z_0^2 - 4C^2 I_0^3 \mu z_0}{4C^2 I_0^3 m z_0} K_\mathrm{d} \tag{9}$$

In the second scenario, the value c will be zero since there will be only two roots, leading to the following condition, which is a vertical line in Figure 3:

$$K_\mathrm{p} = \frac{u_0}{z_0} \tag{10}$$

The requirement for unconditional instability can be determined when the slope of Eq. (9) approaches infinity and coincides with the left vertical line in Figure 3:

$$\mu = \frac{m u_0 z_0}{2CI_0} \tag{11}$$

In the limit where there is no influence of wind ($\mu = 0$), the stability boundary can be derived as:

$$K_\mathrm{p} = \frac{u_0}{z_0} + \frac{u_0 z_0}{2CI_0} K_\mathrm{d} \tag{12}$$

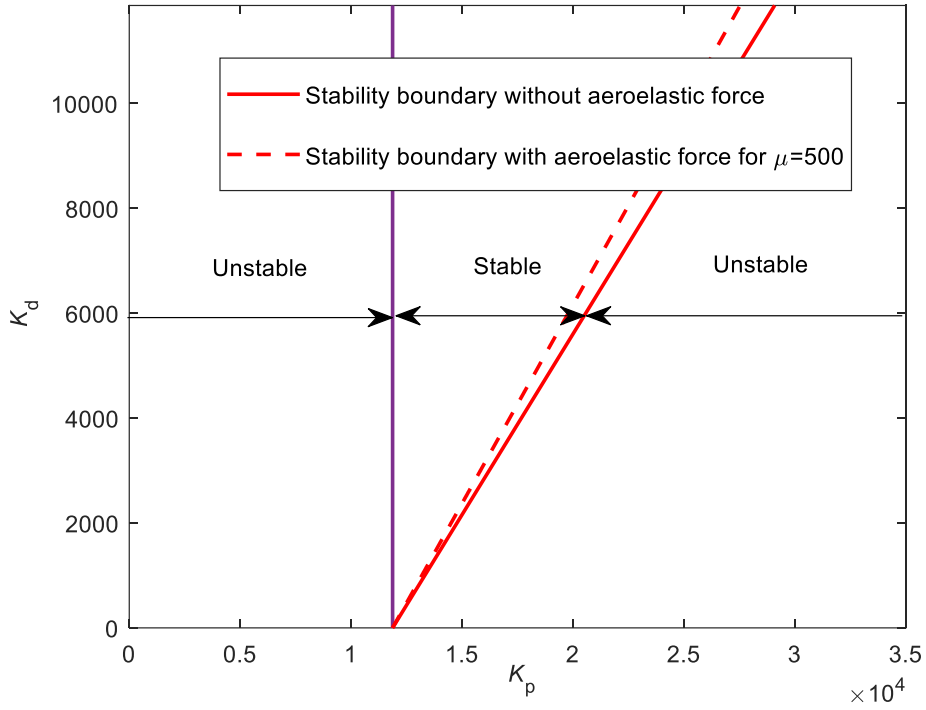

Figure 3: Stability regions for the first fixed point in the K_p - K_d plane. The dashed line represents for the case of galloping. Here, $C = 0.05\left(\mathrm{Nm^2/A^2}\right),\ z_0 = 0.015(\mathrm{m}),\ m = 7650(\mathrm{kg})$

4 Existence of limit cycle for the case $\mu = 0$

The analysis now shifts its focus to the nonlinear dynamics aspects. It is evident from the stability analysis provided earlier that when the real part of the complex conjugates equals zero, the system conducts a harmonic motion (as soon as the motion related to the other root has decayed), typically indicating the presence of a limit cycle in the vicinity. This bears resemblance to the supercritical Hopf bifurcation, albeit typically defined for single-degree-of-freedom systems. We employ the harmonic balance method [10] for this analysis. For simplicity, we truncate after the first harmonics and thus assume that

$$z = z_0 + a\cos(\omega t) \tag{13}$$

$$I = I_0 + b\cos(\omega t) \tag{14}$$

Substituting Eqs. (13) and (14) into (1) and (3), and solving the equation for a, b and ω, the following result is obtained:

$$a = \frac{2\sqrt{2CI_0K_\mathrm{p}z_0 - 2CI_0u_0 - K_\mathrm{d}u_0z_0^2}}{\sqrt{K_\mathrm{d}}\sqrt{u_0}} \tag{15}$$

$$b = \frac{2I_0K_\mathrm{p}\sqrt{-2CI_0u_0 + 2CI_0K_\mathrm{p}z_0 - K_\mathrm{d}u_0z_0^2}}{\sqrt{K_\mathrm{d}}u_0^{3/2}} \tag{16}$$

$$\omega = \frac{I_0\sqrt{K_\mathrm{d}}\sqrt{C\left(K_\mathrm{p}z_0 - u_0\right)}}{\sqrt{mz_0}\sqrt{3CI_0K_\mathrm{p}z_0 - 3CI_0u_0 - K_\mathrm{d}u_0z_0^2}} \tag{17}$$

Eq. (15)-(17) describe the limit cycle for $\mu = 0$.

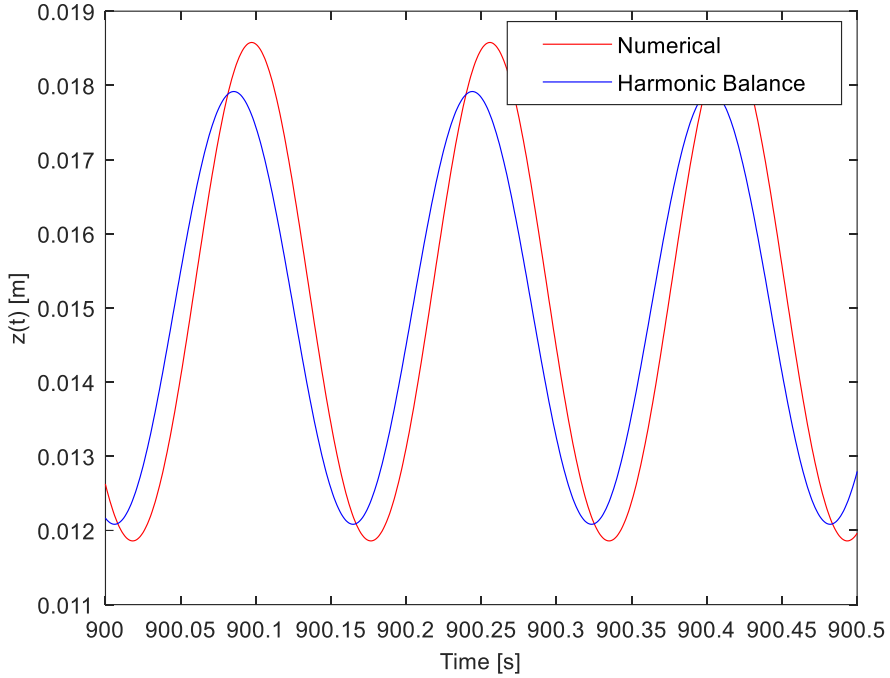

Figure 4. Comparison of numerical integration results and harmonic balance prediction for a limit cycle at $\mu = 0$. Here

$K_\mathrm{p} = 27000\left(\mathrm{V/m}\right), K_\mathrm{d} = 10000\left(\mathrm{Vs/m}\right),\ C = 0.05\left(\mathrm{Nm^2/A^2}\right),\ z_0 = 0.015\left(\mathrm{m}\right),\ m = 7650\left(\mathrm{kg}\right)$.

Results obtained from numerical integration and those from the harmonic balance method are compared in Figure 4. A small error is present due to the neglection of higher harmonics. For the existence of a limit cycle, $a, b, \omega \in \mathbb{R}$ must hold true. The condition derived from this turns out to coincide with the condition previously determined in Eq. (9). In other words, the limit cycle is born right when the fixed point becomes unstable (i.e., at the inclined red line in Figure 3).

5 Conclusion

This study considers the dynamics of a 1.5-degree-of-freedom model consisting of an electromagnetically suspended mass that is excited by the steady aeroelastic force. The model is a simplified representation of a Hyperloop vehicle moving through air. The model allows to derive analytical expressions for stability boundaries by employing linear stability analysis. The results indicate that the control parameter space ($K_p - K_d$) is divided into three distinct regions, one of which exhibits limit cycle behaviour, akin to Hopf bifurcation. The presence of the destabilizing aeroelastic force leads to a marginal reduction in the stable region, with no qualitative changes in the stability landscape. Harmonic balance analysis identifies the region in the control parameter space where the limit cycle exists and provides the amplitudes and frequency for the limit cycle. Future endeavours will delve into examining the influence of the aeroelastic force on the characteristics of the limit cycle.

Acknowledgements

The authors express sincere gratitude to the European Union's Horizon Europe programme for its support through the Marie Skłodowska-Curie grant agreement No 101106482 (HySpeed project).

References

[1] G. G. Denisov, E. K. Kugusheva, and V. V. Novikov, "On the Problem of the Stability of One-Dimensional Unbounded Elastic Systems", Journal of Applied Mathematics and Mechanics **49**, 533, 1985.

[2] A. V. Metrikine, "Unstable Vertical Oscillations of an Object Moving Uniformly along an Elastic Guide as a Result of an Anomalous Doppler Effect", Acoustical Physics **40**, 85, 1994.

[3] Z. Dimitrovová, "On the Critical Velocity of Moving Force and Instability of Moving Mass in Layered Railway Track Models by Semianalytical Approaches", Vibration **6**, 1, 2023.

[4] J. P. D. Hartog, "Mechanical Vibrations", Courier Corporation, 1985.

[5] M. P. Paidoussis, "Fluid-Structure Interactions: Slender Structures and Axial Flow", Academic Press, 1998.

[6] T.-K. Kim, K.-H. Kim, and H.-B. Kwon, "Aerodynamic Characteristics of a Tube Train", Journal of Wind Engineering and Industrial Aerodynamics **99**, 1187, 2011.

[7] Hi. Yabuno, T. Seino, M. Yoshizawa, and Y. Tsujioka, "Dynamical Behavior of a Levitated Body with Magnetic Guides : Parametrically Excitation of the Subharmonic Type Due to the Vertical Motion of Levitated Body", JSME International Journal. Ser. 3, Vibration, Control Engineering, Engineering for Industry **32**, 428, 1989.

[8] T. Inoue and Y. Ishida, "Nonlinear Forced Oscillation in a Magnetically Levitated System: The Effect of the Time Delay of the Electromagnetic Force", Nonlinear Dyn **52**, 103, 2008.
[9] A. B. Fărăgău, A. V. Metrikine, J. Paul, R. van Leijden, K. N. van Dalen, "The interplay between the electro-magnetic and wave-induced instability mechanisms in the Hyperloop transportation system", Preprint submitted to Jorunal of Sound and Vibration.
[10] D. Jordan, P. Smith, D. Jordan, and P. Smith, "Nonlinear Ordinary Differential Equations: An Introduction for Scientists and Engineers", Fourth Edition, Fourth Edition, Oxford University Press, Oxford, New York, 2007.